



Global Pattern Formation and Ethnic/Cultural Violence

May Lim, *et al.*

Science **317**, 1540 (2007);

DOI: 10.1126/science.1142734

The following resources related to this article are available online at www.sciencemag.org (this information is current as of September 21, 2007):

Updated information and services, including high-resolution figures, can be found in the online version of this article at:

<http://www.sciencemag.org/cgi/content/full/317/5844/1540>

Supporting Online Material can be found at:

<http://www.sciencemag.org/cgi/content/full/317/5844/1540/DC1>

This article **cites 20 articles**, 2 of which can be accessed for free:

<http://www.sciencemag.org/cgi/content/full/317/5844/1540#otherarticles>

This article appears in the following **subject collections**:

Sociology

<http://www.sciencemag.org/cgi/collection/sociology>

Information about obtaining **reprints** of this article or about obtaining **permission to reproduce this article** in whole or in part can be found at:

<http://www.sciencemag.org/about/permissions.dtl>

(Fig. 3C). The degeneracy of the effective activation barriers is lifted at high tunneling currents, and based on the Arrhenius-like switching behavior, the mean lifetimes $\bar{\tau}_{0,1}$ can be expressed as (21, 22)

$$\bar{\tau}_{0,1} = \nu_a^{-1} \exp\left[\frac{E_b}{k_B T} \left(1 - \frac{I}{I_c}\right)\right] \quad (1)$$

where ν_a is the attempt frequency, E_b is the effective activation barrier of the island at zero current, k_B is the Boltzmann constant, I denotes the tunneling current, and I_c is the threshold current to switch the magnetization at $T = 0$ K. E_b was determined by a variation of T from 50.6 to 48.5 K and derivation of the respective mean lifetimes $\bar{\tau}_{0,1}$ at low tunneling currents ($I = 1$ nA). For the particular island of Fig. 3, we find $E_b = 133 \pm 4$ meV, leading to a threshold current of $I_c = 89 \pm 4$ μ A. Because such high currents are not realizable within the tunneling regime, we do not expect to switch islands of the given dimensions at $T \approx 0$ K. Assuming an effective tunneling area given by the lateral STM resolution, the corresponding threshold current density is $(113 \pm 5) \times 10^8$ A/cm². This value is, by two to three orders of magnitude, higher than the current density used in similar experiments based on TMR devices (23), which may be attributed to the fact that, in contrast to planar junctions, the current density is not distributed homogeneously on the whole nanoisland but acts very locally. The splitting of the effective activation barrier ΔE due to spin-torque effects can be quantified by

$$\Delta E = k_B T \ln \frac{1 + a_\tau}{1 - a_\tau} \quad (2)$$

where a_τ is the lifetime asymmetry. For $I = 800$ nA, the current-induced spin torque leads to an effective activation barrier splitting of $\Delta E = 1.3 \pm 0.1$ meV, which is only $\approx 1\%$ of E_b .

Using a SP-STM tip as the source or drain for spin-polarized electrons, we were able to perform spatially resolved measurements where the tip is moved to different sites of one particular nanoisland, allowing information of site-specific properties to be gained that cannot be obtained in spatially averaging experiments performed with nanopillars. Figure 4A shows the topography of a nanoisland consisting of about 100 atoms. While scanning this island with $I = 600$ nA, we measured the magnetic dI/dU signal on each of the pixels for a duration of 12 s to calculate the site-specific histogram asymmetry a_H on the basis of the corresponding datapoint histograms. The result is shown in a color-coded representation in Fig. 4B. In spite of the rather large statistical error, a gradient along the [001] direction can clearly be recognized. The effect can even be analyzed quantitatively by averaging a_H column- and row-wise: that is, along the $[1\bar{1}0]$ and the [001] directions, respectively. Whereas \bar{a}_H is constant within the error at about 42% when moving the tip along the $[1\bar{1}0]$ direction, it clearly

reduces by about 16% from the left to the right side of the island. The lateral tip position obviously may influence the switching behavior of the nanoisland at high tunneling currents, as illustrated in Fig. 4, C to E. If the tip is positioned above the island center, the influence of the Oersted field along the $[1\bar{1}0]$ direction, which is the easy axis of the nanoisland, cancels (Fig. 4C). In this case, pure spin-current-induced switching occurs. Likewise, no influence by the Oersted field is expected if the tip is moved from the center to either island edge along the $[1\bar{1}0]$ direction (Fig. 4D) as the effective field acting on the island is oriented perpendicular to the easy axis. Only if the tip is moved from the center along the [001] direction one magnetic state is favored over the other by the Oersted field (Fig. 4E). In this case, Oersted field effects influence the magnetic switching behavior, dependent on the tip position. A detailed analysis of the data yields that the effective activation barrier splitting of $\Delta E = -2.4 \pm 0.2$ meV at the center of the island is increased or decreased by up to 0.7 ± 0.2 meV when moving along the [001] direction to either island edge. This finding indicates that the magnetization switching is dominated by the spin torque induced by the spin-polarized current, whereas the influence of the Oersted field remains small. A simple estimation of the energy splitting caused by the Oersted field, as obtained by integrating the expected field distribution of an infinitely expanded current line over the island area, yields a Zeeman energy of up to $\Delta E_{\text{Oersted}} = \sum \vec{m} \cdot \vec{B}(\vec{r}_i) \approx 0.2$ meV [$|\vec{m}| = 2.79\mu_B$ (24)]¹, where \vec{m} is the magnetic moment, \vec{B} is the Oersted field, \vec{r}_i is the position of atom i , and μ_B is the Bohr magneton. This estimated value is somewhat lower than the experimental result. We attribute the difference to the oversimplified geometry of our model.

Our SP-STM studies provide insight into the details of current-induced magnetization switching that has been inaccessible in experiments

with lithographically fabricated tunnel junctions. The ultimate lateral resolution of SP-STM combined with CIMS promises innovative perspectives for future data storage technologies.

References and Notes

1. J. C. Slonczewski, *J. Magn. Magn. Mater.* **159**, L1 (1996).
2. L. Berger, *Phys. Rev. B* **54**, 9353 (1996).
3. M. Tsoi et al., *Phys. Rev. Lett.* **80**, 4281 (1998).
4. E. B. Myers, D. C. Ralph, J. A. Katine, R. N. Louie, R. A. Buhrman, *Science* **285**, 867 (1999).
5. J. Z. Sun, *J. Magn. Magn. Mater.* **202**, 157 (1999).
6. J. A. Katine, F. J. Albert, R. A. Buhrman, E. B. Myers, D. C. Ralph, *Phys. Rev. Lett.* **84**, 3149 (2000).
7. F. J. Albert, N. C. Emley, E. B. Myers, D. C. Ralph, R. A. Buhrman, *Phys. Rev. Lett.* **89**, 226802 (2002).
8. R. Wiesendanger, *Scanning Probe Microscopy and Spectroscopy: Methods and Applications* (Cambridge Univ. Press, Cambridge, 1994).
9. M. Bode, *Rep. Prog. Phys.* **66**, 523 (2003).
10. J. Tersoff, D. R. Hamann, *Phys. Rev. Lett.* **50**, 1998 (1983).
11. U. Gradmann, G. Liu, H. J. Elmers, M. Przybylski, *Hyperfine Interact.* **57**, 1845 (1990).
12. H. J. Elmers et al., *Phys. Rev. Lett.* **73**, 898 (1994).
13. Y. Acremann et al., *Phys. Rev. Lett.* **96**, 217202 (2006).
14. A. Kubetzka, M. Bode, O. Pietzsch, R. Wiesendanger, *Phys. Rev. Lett.* **88**, 057201 (2002).
15. H. J. Elmers et al., *Phys. Rev. Lett.* **75**, 2031 (1995).
16. M. Bode, O. Pietzsch, A. Kubetzka, R. Wiesendanger, *Phys. Rev. Lett.* **92**, 067201 (2004).
17. M. Bode, A. Kubetzka, K. von Bergmann, O. Pietzsch, R. Wiesendanger, *Microsc. Res. Tech.* **66**, 117 (2005).
18. Supporting materials are available on Science Online.
19. M. P. Seah, W. A. Dench, *Surf. Interface Anal.* **1**, 2 (1979).
20. H. Goldenberg, *Br. J. Appl. Phys.* **3**, 296 (1952).
21. J. Z. Sun, *IBM J. Res. Dev.* **50**, 81 (2006).
22. I. N. Krivorotov et al., *Phys. Rev. Lett.* **93**, 166603 (2004).
23. G. D. Fuchs et al., *Appl. Phys. Lett.* **85**, 1205 (2004).
24. J. Hauschild, H. J. Elmers, U. Gradmann, *Phys. Rev. B* **57**, R677 (1998).
25. Financial support from the Deutsche Forschungsgemeinschaft (SFB668-B4) and the European Union project "Advanced Scanning Probes for Innovative Science and Technology" (ASPRINT) is acknowledged.

Supporting Online Material

www.sciencemag.org/cgi/content/full/317/5844/1537/DC1
SOM Text
Fig. S1

17 May 2007; accepted 26 July 2007
10.1126/science.1145336

Global Pattern Formation and Ethnic/Cultural Violence

May Lim,^{1,2} Richard Metzler,^{1,3} Yaneer Bar-Yam^{1*}

We identify a process of global pattern formation that causes regions to differentiate by culture. Violence arises at boundaries between regions that are not sufficiently well defined. We model cultural differentiation as a separation of groups whose members prefer similar neighbors, with a characteristic group size at which violence occurs. Application of this model to the area of the former Yugoslavia and to India accurately predicts the locations of reported conflict. This model also points to imposed mixing or boundary clarification as mechanisms for promoting peace.

Over the past 100 years, more than 100 million people have died in violent conflicts (1). Of these deaths, a great number are attributable to ongoing local conflict between culturally or ethnically distinct groups. A scientific understanding of the underlying causes of

ethnic violence could lead to policy changes that may help stop or prevent it. The existing literature (2–13) [see also bibliography of ethnic and cultural conflict in the supporting online materials (14)] generally considers (i) the process by which ethno-religious identity is established and if inter-

ventions could diminish its importance relative to more inclusive identities, and (ii) control mechanisms of the state and of organizations of ethnic groups and if interventions could strengthen the state while subsuming or accommodating ethnic groups within state authority. More specific social and economic factors identified in the literature as contributing to violence include oppression of minorities, economic grievances, historical precedents, competition for resources, favoritism, availability of resources for violence, security fears, mobilization by elites, weak social ties, national ethnic diversity, territorial claims, religious or political polarization, incendiary media, and international influences. Although most of these studies consider national conditions, a few consider local violence to identify the role of local socio-economic or geographic factors (7–9). Here, we focus on an aspect of spatial population structure that has been neglected so far; we analyze the global pattern of violence and propose that many instances are consistent with the natural dynam-

ics of type separation (15–18), a form of pattern formation (19) also seen in physical or chemical phase separation. Violence arises due to the structure of boundaries between groups rather than as a result of inherent conflicts between the groups themselves. In this approach, diverse social and economic causal factors trigger violence when the spatial population structure creates a propensity to conflict, so that spatial heterogeneity itself is predictive of local violence. The local ethnic patch size serves as an “order parameter,” a measure of the degree of order of collective behavior, to which other aspects of behavior are coupled. The importance of collective behavior implies that ethnic violence can be studied in the universal context of collective dynamics, where models can identify how individual and collective behavior are related.

A simple model of type separation is shown in Fig. 1, A to E. The dynamics of this model assume that individuals preferentially move to areas where more individuals of the same type reside (14). The resulting dynamics lead to progressively larger patches (“islands” or “peninsulas”) of each type. The average size of patches at a particular time can be obtained by a number of different methods. We used overlapping spatial waves that represent the spatial variation of the population density. Each wave makes a contribu-

tion proportional to its correlation with the population density (the structure factor or Fourier transform). The wavelength of the wave that has the maximum amplitude gives the average size of the patches. Other methods of obtaining the size of patches give similar results. The size of the patches grows as a characteristic power of time (Fig. 1F, inset). This behavior has been proven (20) to be a “universal behavior” that does not depend on many of the details of the model and therefore may be relied on to describe a large variety of systems of interacting elements; in particular, similar models have been used to describe the relation of chemical interaction energies and chemical precipitation or phase separation (21, 22). The universal properties of the patterns upon rescaling of length and time also imply that a number of individual agents of the model can be aggregated into a single agent if time is rescaled correspondingly without changing the behavior at the larger scales (Fig. 1F). Thus, it is possible to consider a model agent to represent a local population, and it is not necessary to model the behavior of each individual—an impractical undertaking.

To model violence, we assume that highly mixed regions do not engage in violence, and neither do well-segregated groups, an intuitive hypothesis with empirical support (7). The analy-

¹New England Complex Systems Institute, 24 Mt. Auburn Street, Cambridge, MA 02138, USA. ²Brandeis University, Waltham, MA 02454, USA. ³Massachusetts Institute of Technology, Cambridge, MA 02139, USA.

*To whom correspondence should be addressed. E-mail: yaneer@necci.edu

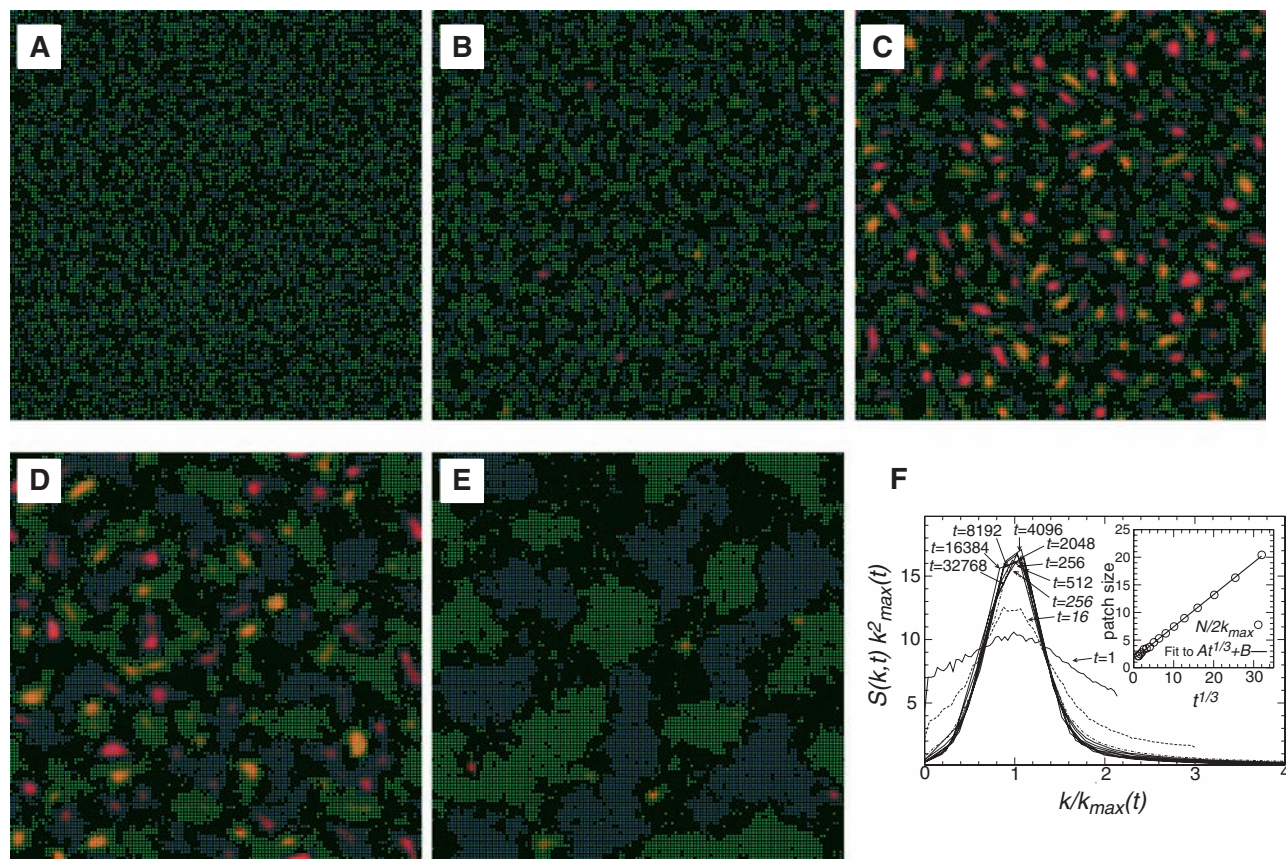


Fig. 1. Simulation of type separation with two types of agents [(A) to (E) show the system at 8, 64, 512, 4096, and 32768 attempted moves per particle, respectively]. The shape of domains (as characterized by the rescaled structure factor amplitude squared) remains constant after an initial transient (F), and

the average size of clusters grows as a power law [inset of (F)] (14). Patches of a certain size that are surrounded by the other type are highlighted by red shading overlay in (A) to (E). We identify such regions with a high likelihood of conflict.

sis is applicable to communal violence and not to criminal activity or interstate warfare. In highly mixed regions, groups of the same type are not large enough to develop strong collective identities, or to identify public spaces as associated with one or another cultural group. They are neither imposed upon nor impose upon other groups, and are not perceived as a threat to the cultural values or social/political self-determination of other groups. Partial separation with poorly defined boundaries fosters conflict. Violence arises when groups are of a size that they are able to impose cultural norms on public spaces, but where there are still intermittent violations of these rules due to the overlap of cultural domains. When groups are larger than the critical size, they typi-

cally form self-sufficient entities that enjoy local sovereignty. Hence, we expect violence to arise when groups of a certain characteristic size are formed, and not when groups are much smaller or larger than this size. The model of violence depends on the distribution of the population and not on the specific mechanism by which the population achieves this structure, which may include internally or externally directed migrations. By focusing on the geographic distribution of the population, the model seeks a predictor of conflict that can be easily determined by census. This may work well because geography is an important aspect of the dimensions of social space, the dynamic coarsening process is universal, and other aspects of social behavior (e.g., isolation-

ism, conformity, as well as violence) are correlated to it.

The predictor that we identify based on spatial census data need not describe the immediate social or institutional triggers of violence, only the conditions under which violence becomes likely. Previous research aiming to characterize ethnic conflict by census data has focused on measures of ethnic or religious “fragmentation” (23–27). Such measures characterize the diversity of a country without reference to its spatial structure, i.e., the overall proportions of ethnically distinct groups in a country. They are therefore distinct from the spatial characterization of our study. The literature is divided about whether or which correlations exist with measures of national ethnic composition. We

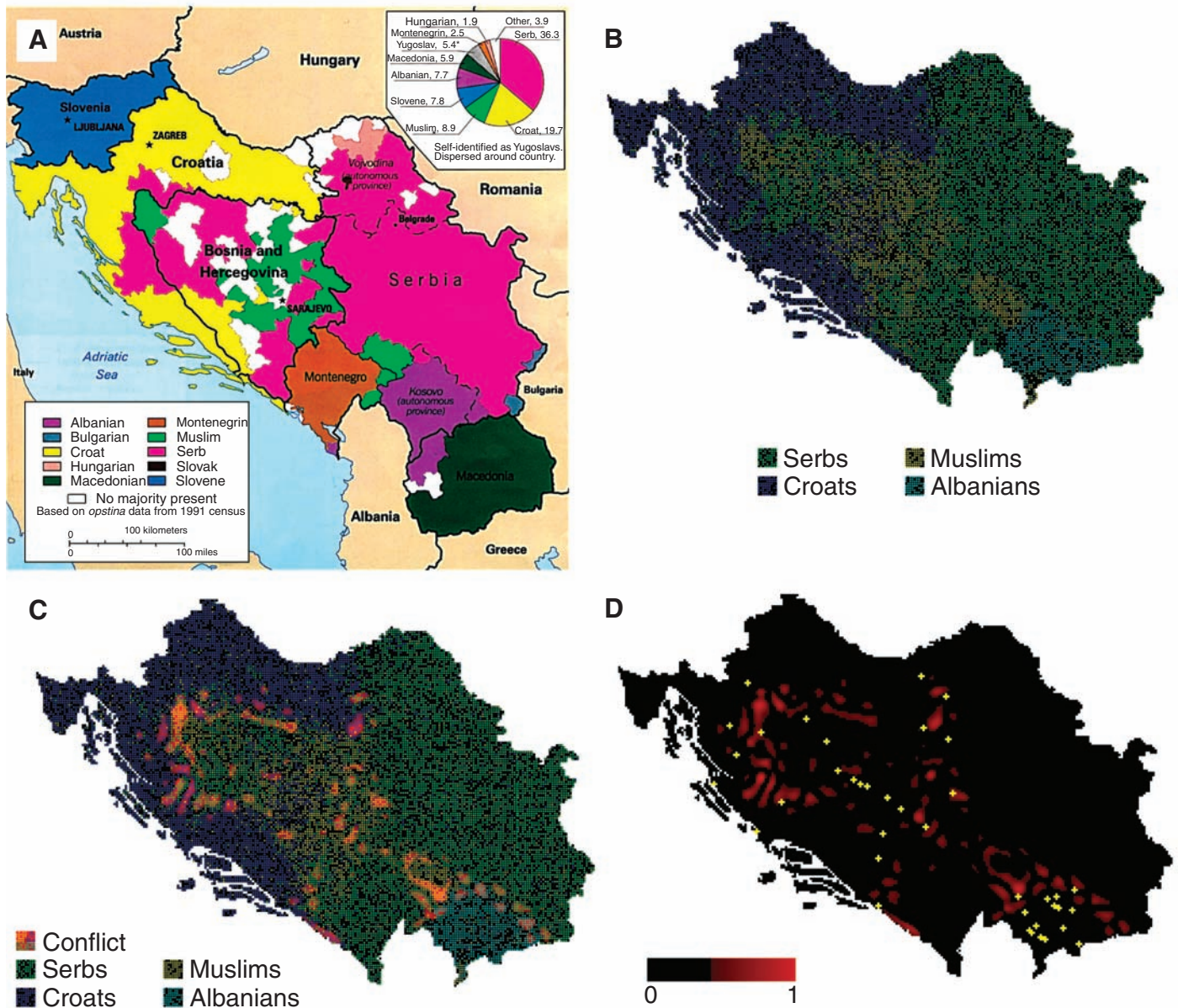


Fig. 2. (A) Census data from 1991 shown here in map form were converted into a spatial representation and used in an agent-based simulation shown in (B). Our prediction of populations likely to be

in conflict with neighboring groups [red overlay, (C) and (D)] agrees well with the location of cities reported as sites of major fights and massacres [yellow dots, (D)].

find, however, that the spatial distribution of ethnic groups is a strong predictor of locations of violence.

Mathematically, the expected violence was determined by detecting patches consisting of islands or peninsulas of one type surrounded by populations of other types. We detected these features by correlation of the population for each population type with a template that has a positive center and a negative surround. To illustrate the effect of this correlation, for a particular template size, the maximum correlation over population types is superimposed as a red overlay in Fig. 1, A to E. Over time in this simulation, the patch size starts smaller, then passes through and becomes larger than the template size chosen. The specific template that we used is based on a wavelet filter (14, 28–30). Wavelets are designed to obtain a local measure of the degree to which a certain scale of variation (wavelength) is present. Outcomes are highly robust, and other templates give similar results. Given the universality of the dynamic behavior, the diameter of the positive region of the wavelet, i.e., the size of the local population patches that are likely to experience violence, is the only essential parameter of the model. The parameter is to be determined by agreement of the model with reports of violence, though as we will see, the agreement is robust to variation of the parameter. The quality of the agreement provides a measure of the validity of the model.

To test the predictive ability of the model, we performed simulations based on census data for the former Yugoslavia and India. We assigned areas of pixelated geographic maps pixel by pixel to ethnic groups at random, but in proportion to their relative population census in the region. Although this does not reflect the physical geography or local mixing of

groups in buildings and villages, over an area of multiple pixels it captures the regional composition of the census. The pixelated map serves as the beginning state for the agent model. For Yugoslavia, census data from the early 1990s before the outbreak of conflict (31, 32), as shown in Fig. 2A, were captured into an agent simulation (Fig. 2B), which was used to obtain the regions of expected violence shown in Fig. 2C.

We then obtained from books (2), newspapers, and Internet sources (see supporting online text) the locations of reported violence for the area of the former Yugoslavia. Multiple independent sources were used to provide validation for each location of violence (14). We consider these reports as indicators of areas of actual violence, keeping in mind possible bias and incompleteness and that areas of widespread violence are identified only by local urban centers. In comparing such reports with model predictions, we note that the model identifies locations of groups of a particular size, but the location of the actual violence should occur somewhere in the area between adjacent groups. Despite these caveats, overlaying the locations of reported and predicted violence in Fig. 2D demonstrates a significant ability of our simple model to identify regions of reported violence. We performed statistical analyses comparing the predicted to the reported violence, evaluating the ability of the model to determine both where violence occurs and where violence does not occur. For comparison, we randomized the locations of reported violence. We defined “conflict proximity” as the distance between a given position and the nearest location of violence (predicted, reported, or randomized). We calculated Pearson's correlation and other statistical measures between the proximities of predicted and reported

violence, and compared them with the same measures in relation to randomized reports. We found that the model has a correlation of 0.9 with reports (0.89 to two significant digits), a level of agreement not reached in any of 100,000 randomized trials. Moreover, the predicted results are highly robust to parameter variation, with essentially equivalent agreement obtained for filter diameters ranging from 18 to 60 km, a range that is in agreement with intuition about the size of conflict areas. Below or above this range, poorer agreement occurs. Details are provided in the supporting online text.

We studied conflict in India as a second case study of the ethnic violence model. We constructed a spatial representation of India on a district level from maps at www.censusindia.net and obtained the distribution of ethno-cultural groups from the 2001 Census data at www.indiastat.com. The result can be seen in the form of three-color maps in Fig. 3, A and B, representing the relative densities of Hindus, Muslims, Christians, Sikhs, Buddhists, and Others (primarily Jains). The agent model is shown in Fig. 3C and the prediction of ethnic violence is indicated in Fig. 3D. Predictions correspond very well to the primary locations of “extremist” violence of government reports as given by indiastat.com (Fig. 3E) and confirmed by independent sources (14), particularly in Kashmir, Punjab, and the states of Northeast India. Some additional areas of lesser violence were also predicted by the model, particularly Jharkhand—an eastern state created in 2000 that has recently experienced some violence (14, 33). Consistent with predicted results, the violence in this region is not as prevalent as in other violence-prone areas of India. Statistical correlation measures of conflict proximity yield a correlation of 0.998 when the threshold is set above the value of predicted violence in Jharkhand. If the threshold is set lower, so that violence in Jharkhand is included in predicted but not in reported cases, the correlation falls to 0.92. Including reported violence in Jharkhand when comparing at the lower threshold increases the correlation to 0.98. Additional details are provided in the supporting online text. The range of filter diameter values for which good agreement was obtained overlaps that of the former Yugoslavia. However, it is shifted to larger values, up to ~100 km. This may reflect not only the larger granularity of data, but perhaps also the effect of violence itself on separation. Unlike Yugoslavia, in India the census was performed during ongoing violence. Because violence accelerates the process of separation, groups in conflict are likely to have separated substantially and reflect the high end of group sizes susceptible to violence.

Governmental and nongovernmental organizations are devoting increasing attention to the prevention of major conflict (34). Under some circumstances, social and institutional factors that affect violence might serve to suppress the triggering of violence without changing the spatial structure of the population. However, influencing the spatial structure might address the conditions that promote violence described here. Such ap-

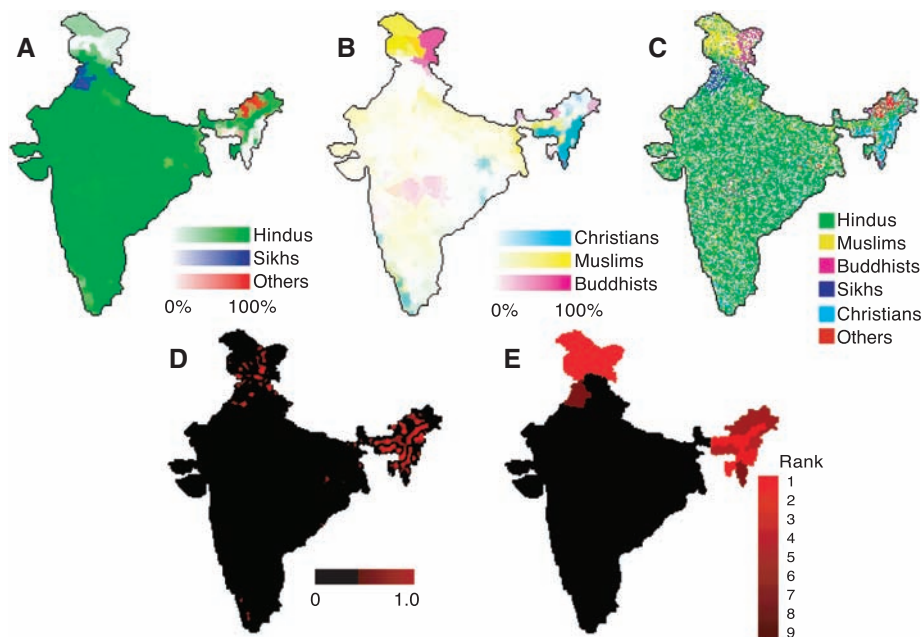


Fig. 3. (A and B) Spatial representation of Indian census data from 2001 of six indicated groups was converted into an agent-based simulation shown in (C). Our prediction of conflict-prone areas [red areas in (D)] agrees with states where major ethnic violence has been reported [red areas in (E)] between 1999 and 2002, with the red shading intensity corresponding to the rank order of states by number of incidents.

proaches have been and are being considered. For example, in Singapore, where 84% of the population lives in public housing (35), regulations that explicitly recognize the role of spatial segregation in sectarianism specify the percentage of ethnic groups to occupy housing blocks (36). This legally compels ethnic mixing at a scale finer than that which our study finds likely to lead to violence. Given the natural tendency toward social separation, maintaining such mixing requires a level of authoritarianism that might not be entertained in other locations. Still, despite social tensions (37), the current absence of violence provides some support to our analysis. The alternative approach—aiding in the separation process by establishing clear boundaries between cultural groups to prevent violence—has also gained recent attention (38, 39). Although further studies are needed, there exist assessments (39) of the impact of historical partitions in Ireland, Cyprus, the Indian subcontinent, and the Middle East that may be consistent with the understanding of type separation and a critical scale of mixing or separation presented here.

The insight provided by this study may help inform policy debates by guiding our understanding of the consequences of policy alternatives. The purpose of this paper does not include promoting specific policy options. Although our work reinforces suggestions to consider separation, we are not diminishing the relevance of concerns about the desirability of separation or its process. Even where separation may be indicated as a way of preventing violence, caution is warranted to ensure that the goal of preventing violence does not become a justification for violence. Moreover, even a peaceful process of separation is likely to be objectionable. There may be ways to positively motivate separation using incentives, as well as to mitigate negative aspects of separation that often include displacement of populations and mobility barriers.

Our results for the range of filter diameters that provide good statistical agreement between reported and predicted violence in the former Yugoslavia and India suggest that regions of width less than 10 km or greater than 100 km may provide sufficient mixing or isolation to reduce the chance of violence. These bounds may be affected by a variety of secondary factors including social and economic conditions; the simulation resolution may limit the accuracy of the lower limit; and boundaries such as rivers, other physical barriers, or political divisions will surely play a role. Still, this may provide initial guidance for strategic planning. Identifying the nature of boundaries to be established and the means for ensuring their stability, however, must reflect local issues.

Our approach does not consider the relative merits of cultures, individual acts, or immediate causes of violence, but rather the conditions that may promote violence. It is worth considering whether, in places where cultural differentiation is taking place, conflict might be prevented or minimized by political acts that create appropriate boundaries suited to the current geocultural regions rather than the existing

historically based state boundaries. Such boundaries need not inhibit trade and commerce and need not mark the boundaries of states, but should allow each cultural group to adopt independent behaviors in separate domains. Peaceful coexistence need not require complete integration.

References and Notes

1. M. White, *Deaths by Mass Unpleasantness: Estimated Total for the Entire 20th Century*, <http://users.erols.com/mwhite28/warstat8.htm> (September 2005).
2. D. L. Horowitz, *Ethnic Groups in Conflict* (Univ. of California Press, Berkeley and Los Angeles, ed. 2, 2000).
3. B. Harff, T. R. Gurr, *Ethnic Conflict in World Politics* (Westview, Boulder, ed. 2, 2004).
4. S. Huntington, *The Clash of Civilizations and the Remaking of World Order* (Simon & Schuster, New York, 1996).
5. D. Chiro, M. E. P. Seligman, Eds., *Ethnopolitical Warfare: Causes, Consequences, and Possible Solutions* (American Psychological Association, Washington, DC, 2001).
6. M. Reynal-Querol, *J. Conflict Resolut.* **46**, 29 (2002).
7. T. R. Gulden, *Politics Life Sciences* **21**, 26 (2002).
8. H. Buhaug, S. Gates, *J. Peace Res.* **39**, 417 (2002).
9. A. Varshney, *Ethnic Conflict and Civic Life: Hindus and Muslims in India* (Yale Univ. Press, New Haven, CT, 2003).
10. M. D. Toft, *The Geography of Ethnic Violence: Identity, Interests, and the Indivisibility of Territory* (Princeton Univ. Press, Princeton, NJ, 2003).
11. J. Fox, *Religion, Civilization, and Civil War: 1945 through the New Millennium* (Lexington Books, Lanham, MD, 2004).
12. M. Mann, *The Dark Side of Democracy: Explaining Ethnic Cleansing* (Cambridge Univ. Press, New York, 2004).
13. I. Lustick, *Am. Polit. Sci. Rev.* **98**, 209 (2004).
14. Materials and methods are available as supporting material on Science Online.
15. T. C. Schelling, *J. Math. Sociol.* **1**, 143 (1971).
16. J. Mimkes, *J. Therm. Anal.* **43**, 521 (1995).
17. H. P. Young, *Individual Strategy and Social Structure* (Princeton Univ. Press, Princeton, NJ, 1998).
18. R. Van Kempen, A. S. Ozuekren, *Urban Stud.* **35**, 1631 (1998).
19. Y. Bar-Yam, in *Dynamics of Complex Systems* (Perseus Press, Cambridge, MA, 1997), chap. 7.
20. A. J. Bray, *Adv. Phys.* **43**, 357 (1994).
21. I. M. Lifshitz, V. V. Slyozov, *J. Phys. Chem. Solids* **19**, 35 (1961).
22. D. A. Huse, *Phys. Rev. B* **34**, 7845 (1986).
23. W. Easterly, R. Levine, *Q. J. Econ.* **112**, 1203 (1997).
24. P. Collier, A. Hoeffler, *Oxf. Econ. Pap.* **50**, 563 (1998).
25. R. H. Bates, *Am. Econ. Rev.* **90**, 131 (2000).
26. J. D. Fearon, D. D. Laitin, *Am. Pol. Sci. Rev.* **97**, 75 (2003).
27. D. N. Posner, *Am. J. Pol. Sci.* **48**, 849 (2004).
28. I. Daubechies, *Ten Lectures on Wavelets*, (SIAM, Philadelphia, 1992).
29. A. Arneodo, E. Bacry, P. V. Graves, J. F. Muzy, *Phys. Rev. Lett.* **74**, 3293 (1995).
30. P. Ch. Ivanov *et al.*, *Nature* **383**, 323 (1996).
31. Map of Yugoslavia, Courtesy of the University of Texas Libraries., www.lib.utexas.edu/maps/europe/yugoslav.jpg.
32. R. Petrovic, *Yugosl. Surv.* **33**, 3 (1992).
33. K. Chaudhuri, *Frontline* **18** (no. 2), www.hinduonnet.com/line/fl1802/18020330.htm.
34. *Final Report*, Carnegie Commission on Preventing Deadly Conflict, www.wilsoncenter.org/subsites/ccpcd/pubs/rept97/finr.htm.
35. *A Brief Background*, Housing and Development Board, Singapore Government, www.hdb.gov.sg/ff10/ff10296p.nsf/WPDis/About%20UsA%20Brief%20Background%20-%20HDB's%20Beginnings.
36. Ethnic Integration Policy, Housing and Development Board, Singapore Government, www.hdb.gov.sg/ff10/ff10201p.nsf/WPDis/Buying%20A%20Resale%20FlatEthnic%20Group%20Eligibility.
37. D. Murphy, *Christian Science Monitor*, 5 February 2002, www.csmonitor.com/2002/0205/p07s01-woap.html.
38. J. Tullberg, B. S. Tullberg, *Politics Life Sciences* **16**, 237 (1997).
39. C. Kaufmann, *Int. Secur.* **23**, 120 (1998).
40. We thank G. Wolfe, M. Woolsey, and L. Burlingame for editing the manuscript; B. Wang for assistance with figures; M. Nguyen and Z. Bar-Yam for assistance with identifying data; and I. Epstein, S. Pimm, F. Schwartz, E. Downs, and S. Frey for helpful comments. We acknowledge internal support by the New England Complex Systems Institute and the U.S. government for support of preliminary results.

Supporting Online Material

www.sciencemag.org/cgi/content/full/317/5844/1540/DC1
Methods
Figs. S1.1 to S4.3
SOM Text
Table S1
References
Bibliography
30 November 2006; accepted 13 August 2007
10.1126/science.1142734

Crystal Structure of an Ancient Protein: Evolution by Conformational Epistasis

Eric A. Ortlund,^{1*} Jamie T. Bridgman,^{2*} Matthew R. Redinbo,¹ Joseph W. Thornton^{2†}

The structural mechanisms by which proteins have evolved new functions are known only indirectly. We report x-ray crystal structures of a resurrected ancestral protein—the ~450 million-year-old precursor of vertebrate glucocorticoid (GR) and mineralocorticoid (MR) receptors. Using structural, phylogenetic, and functional analysis, we identify the specific set of historical mutations that recapitulate the evolution of GR's hormone specificity from an MR-like ancestor. These substitutions repositioned crucial residues to create new receptor-ligand and intraprotein contacts. Strong epistatic interactions occur because one substitution changes the conformational position of another site. "Permissive" mutations—substitutions of no immediate consequence, which stabilize specific elements of the protein and allow it to tolerate subsequent function-switching changes—played a major role in determining GR's evolutionary trajectory.

A central goal in molecular evolution is to understand the mechanisms and dynamics by which changes in gene sequence generate shifts in function and therefore phenotype (1, 2). A complete understanding of this

process requires analysis of how changes in protein structure mediate the effects of mutations on function. Comparative analyses of extant proteins have provided indirect insights into the diversification of protein structure (3–6), and protein